Synchrotron beamline optics for X-ray powder diffraction under high-pressure conditions at the Siam Photon Laboratory

V. Saengsuwan[1,*], W. Klysubun[2], T. Bovornratanaraks[1], S. Rugmai[2]

[1] Department of Physics, Chulalongkorn University, Bangkok, Thailand
[2] Synchrotron Light Research Institute, Nakorn Ratchasima, Thailand
[*] varalak.s@student.chula.ac.th

Keywords: X-ray powder diffraction, diamond anvil cell, high-pressure conditions

Abstract. To support various applications for high-pressure research in Thailand, an experimental setup for X-ray powder diffraction under high-pressure conditions using synchrotron radiation, which is based on station 9.1 at the Daresbury Synchrotron Radiation Source, is being developed on the bending magnet beamline BL8 at the Siam Photon Laboratory. Monochromatic X-rays with a photon energy of 9 keV are provided by a fixed-exit double crystal monochromator equipped with Ge(220) crystals. In a recent experiment, we could record a complete diffraction pattern of the hexagonal phase of ZnO using an image plate area detector. However, diffraction intensity should be improved by adding focusing optics. In this work, we propose the use of a double multilayer monochromator in combination with a focusing mirror. Results from ray-tracing simulation for the proposed optics will be presented.

Introduction

Nowadays, the study of structural phase transitions in materials under high-pressure conditions plays an important role in expanding the understanding of physical and chemical properties of materials. To support various applications for high-pressure research in Thailand, an experimental setup for X-ray powder diffraction (XRPD) under high-pressure conditions using synchrotron radiation, which is based on station 9.1 at the Daresbury Synchrotron Radiation Source [1], is being developed on the bending magnet beamline BL8 of the Siam Photon Laboratory (SPL) [2]. Monochromatic X-rays with a photon energy of 9 keV are provided by a fixed-exit double crystal monochromator equipped with Ge(220) crystals. A diamond anvil cell (DAC) will be used for generating high-pressure conditions in a powder sample. Quasi-hydrostatic pressure in the DAC will be determined by the ruby-fluorescence technique. In our recent work, we can record the complete diffraction pattern of the hexagonal phase of ZnO at BL8 using an image plate area detector. However, the diffraction intensity would have been stronger if there were focusing optics to converge the whole X-ray beam onto the sample. In addition, some intensity loss by X-ray absorption in the DAC at 9 keV is expected. This can be compensated by higher flux. Here we propose an XRPD beamline to deliver a focused X-ray beam with high photon flux as shown in figure 1. Expected performance of the proposed XRPD beamline was determined by ray-tracing simulation with the aid of SHADOW [3]. The X-ray beam simulated for the bending magnet source was traced through each optic and characterized in terms of photon flux, beam size, beam convergence and energy resolution. As compared to a Ge(220) double crystal monochromator (DCM) used at BL8 of the SPL [4], higher photon flux can be obtained from a double multilayer monochromator (DMM), which plays a vital role in the high flux applications, for example, XRPD technique, microscopic X-ray fluorescence analysis, small-angle X-ray scattering technique and X-ray topography [5]. We consider a W/B_4C DMM [6-9] that is employed in a superconducting bending magnet beamline for high-pressure studies at the Advanced Light Source [10] and a microscopic XRD at HASYLAB [11].

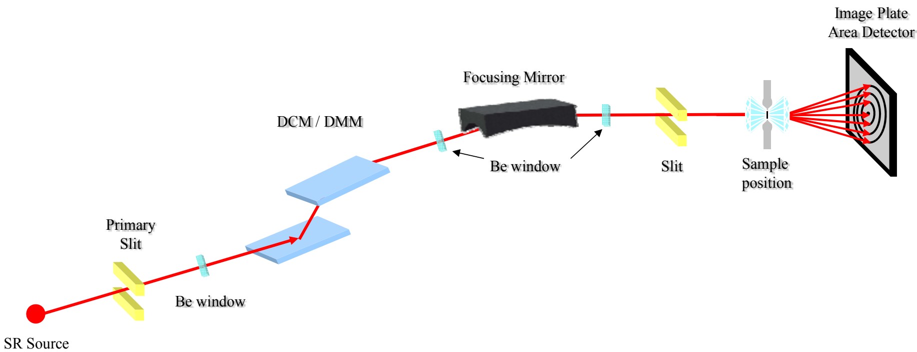

Figure 1. Schematic layout of the proposed XRPD beamline for the SPL.

Beamline Optics

Double Multilayer Monochromator

A W/B_4C multilayer (ML) with a small double layer period (d-spacing) of 10 Å, 600 layer pairs and a ratio of metal to double layer thickness (Γ) of 0.5 is selected for this XRPD beamline. The fabrication and characterization of this mirror was reported by S. Braun *et al.* [12]. Figure 2(a) shows a comparison of the simulated photon flux from the Ge(220) DCM and from the W/B_4C DMM. In overall, the W/B_4C DMM provides photon flux about 46 times higher than that of the Ge(220) DCM. This is mainly attributed to the larger natural bandwidth of the W/B_4C DMM. At 9 keV, the bandwidth of the W/B_4C DMM is 86.0 arcsec while that of the Ge(220) crystal is only 11.8 arcsec. The opening angle of 3.0(h)×0.417(v) $mrad^2$, which was defined by the primary slit (see figure 1), was selected for calculating the photon flux given by the W/B_4C DMM. The vertical angle was set equal to the W/B_4C bandwidth and the horizontal angle was selected to match the width of the focusing mirror as described in section "Focusing Mirror". In case of the Ge(220) DCM the opening angle of 1.75(h)×0.125(v) $mrad^2$ is normally used at the BL8. The reflectivity of the W/B_4C ML for different photon energies as a function of glancing angle is presented in figure 2(b). The rocking curve in figure 3 shows the bandwidth of 86.0 arcsec for W/B_4C ML tuned at 9 keV.

This corresponds to an energy resolution ($\Delta E/E$) of 6.0 $\times 10^{-3}$. It should be noted that the W/B_4C DMM yields higher flux than Ge(220) DCM at the cost of energy resolution.

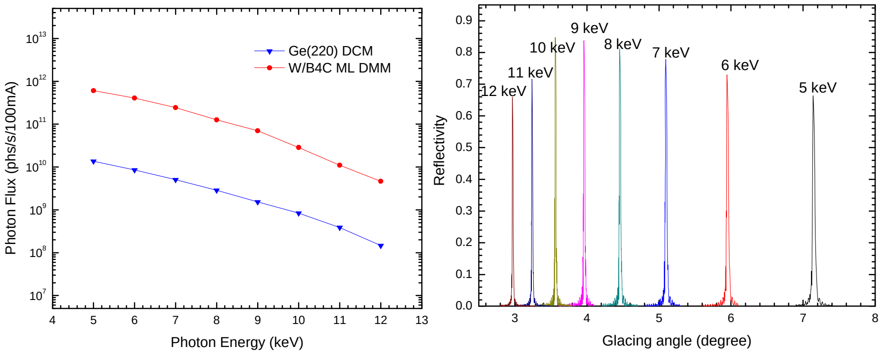

(a) *(b)*

Figure 2. Comparison of simulated photon flux between the Ge(220) DCM and the W/B_4C DMM for photon energies range of 5-12 keV is shown in (a). Reflectivity of the W/B_4C ML with d-spacing 10 Å, N=600 bi-layers and $\Gamma = 0.5$ at photon energies of 5, 6, 7, ..., 12 keV is shown in (b).

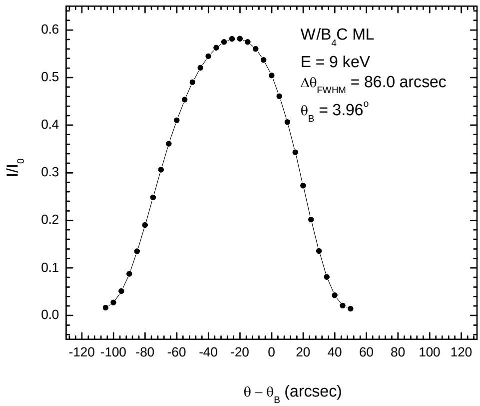

Figure 3. Simulated rocking curve for the DMM with W/B_4C ML at 9 keV.

Focusing Mirror

The focusing mirror is a toroidal mirror or a bent cylindrical mirror as illustrated in figure 4(a) with a meridional radius R for focusing the beam in the horizontal (x) direction and a sagittal radius ρ for focusing the beam in the vertical (z) direction with respect to the optical axis (y) of the x-ray beam. To determine both R and ρ, the optical magnifications are selected such that the focused beam size and beam convergence at the image (sample position) are suitable for XRPD technique. The optical magnifications of the beamline optics are illustrated in figure 4(b). The horizontal magnification and the vertical magnification (M) are given by the ratio of the source and the image plane distances as equivalent to the beam convergence ratio. In addition, the mirror absorption is of considerably importance. We choose

Rh 5 nm/ Pt 25 nm for optical coating on the mirror. The mirror body may be silicon single crystal or ultra low expansion (ULE) fused silica. The suitable glancing angle (θ_c) for the XRPD technique in photon energies range of 5-12 keV is 5 mrad. This is shown in figure 5. For the same length of the mirror, i.e. 1 m, the mirror set at 3 mrad glancing angle accepts 30% less of the beam than in the case of 5 mrad with slightly higher reflectivity, thus the overall beam intensity throughput of 3 mrad is lower than that of 5 mrad.

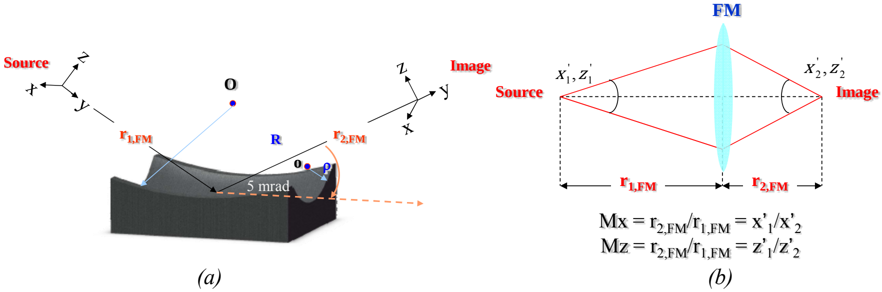

Figure 4. Schematic diagram of focusing mirror and the optical magnifications.

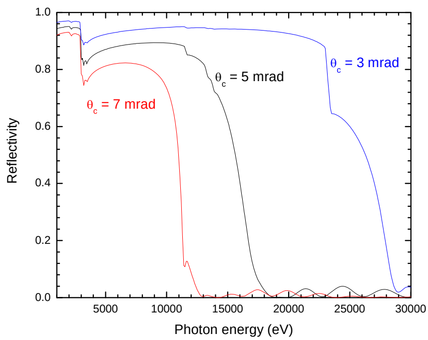

Figure 5. Calculated reflectivity of Rh 5 nm/ Pt 25 nm coated silicon mirror with θ_c = 3, 5 and 7 mrad.

Results and discussions

In order to determine the best magnification of the toroidal focusing mirror, ray-tracing simulation was carried out with the aid of SHADOW. A primary X-ray beam from a bending magnet synchrotron source was generated at 2% bandwidth with energy centred at 9 keV. Different mirror magnifications – M0.3, M0.4, M0.5, M0.6 and M0.7 – allowed by the available length of the beamline, 19 m, were tested with the opening angle of 3.0(h)×0.417(v) $mrad^2$. The X-ray beam at the image plane could be characterized by the beam size, beam convergence and beam intensity. The results including a photon flux and the image size at focal plane of the X-ray beam from ray-tracing simulation are presented in figures 6 and 7. The photon flux at the sample for M0.7 is highest. Moreover, the focused beam size is smallest and spatially symmetric. The expected flux at the sample through a 0.3×0.3 mm^2 aperture is 2.7×10^{10} photons/sec/100mA and without aperture is 5.9×10^{10} photons/sec/100mA. For M0.7, the distances from source to the DMM and to the focusing mirror are 9.83 m and 11.18 m respectively.

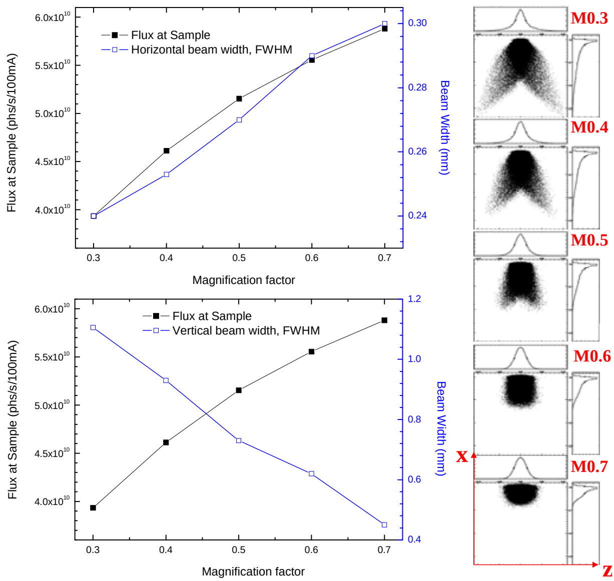

Figure 6. Image size at focal plane for the mirror magnifications M0.3, M0.4, M0.5, M0.6 and M0.7. Right panel shows spatial distribution (scattered plots) and intensity profiles (histograms) of the focused beams. x and z refer to horizontal and vertical directions of the focused beam with respect to the optical axis.

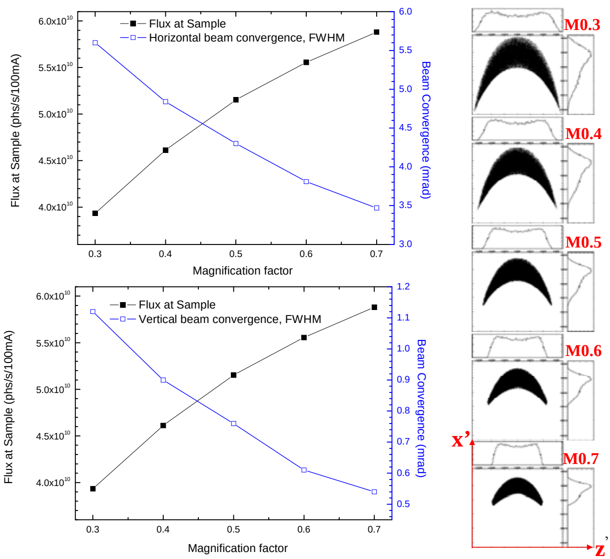

Figure 7. Beam convergence at focal plane for the mirror magnifications M0.3, M0.4, M0.5, M0.6 and M0.7. Right panel shows angular distribution (scattered plots) and intensity profiles (histograms) of the focused beams. x' and z' refer to convergent angles in sagital and meridional plans of the mirror.

Conclusions

At this point, we can conclude that the W/B_4C multilayer is appropriate for the DMM in order to increase the photon flux for the bending magnet beamline at the SPL. The optimal mirror magnification of the toroidal focusing mirror for the limited length of the beamline is M0.7. The expected flux at the sample through a 0.3×0.3 mm^2 aperture is about 7500 times higher than that of BL8 currently. In addition, a low level of aberration and a small X-ray beam size are required for the XRPD technique. Therefore, the mirror magnification of M0.7 is a good choice for upgrading the existing beamline or developing a new one.

References

1. Bovornratanaraks, T., 2001, *Ph.D. Thesis* (The University of Edinburgh).
2. National Synchrotron Research Center, 2006, *Annual Report* (Thailand: Gnomes House Co., Ltd.).
3. Welnak, C., Chen, G.J. & and Cerrina, F., 1994, *Nucl. Instrum. Methods Phys. Res. A*, **347**, 344.
4. Klysubun, W., Sombunchoo, P., Wongprachanukul, P., Tarawarakarn, P., Klinkhieo, S., Chaiprapa, J. & Songsiriritthigul, P., 2007, *Nucl. Instrum. Methods Phys. Res. A*, **582**, 87.
5. Riesemeier, H., Ecker, K., Görner, W., Müller, B.R., Radtke, M. & Krumrey, M., 2005, *X-Ray Spectrom.*, **34**, 160.
6. Shvyd'ko, Y., 2004, *X-Ray Optics: High-Energy-Resolution Applications* (Springer Series in Optical Sciences), (Berlin, Heidelberg: Springer-Verlag).
7. A. Kazimirov, A., Smilgies, D.M., Shen, Q., Xiao, X., Hao, Q., Fontes, E., Bilderback, D.H., Gruner, S.M., Platonovb, Y. & Martynovb, V.V., 2006, *J. Synchr. Rad.*, **13**, 204.
8. Morawe, C., Peffen, J.C., Ziegler, E. & Freund, A.K., 2001, *SPIE Proceedings*, **4145**, 61.
9. Salashchenko, N.N., Platonov, Y.Y. & Zuev, S.Y., 1995, *Nucl. Instrum. Methods Phys. Res. A*, **359**, 114.
10. Kunz, M., MacDowell, A.A., Caldwell, W.A., Cambie, D., Celestre, R.S., Domning, E.E., Duarte, R.M., Gleason, A.E., Glossinger, J.M., Kelez, N., Plate, D.W., Yu, T., Zaug, J.M., Padmore, H.A., Jeanloz, R., Alivisatos, A.P. & and Clark, S.M., 2005, *J. Synchr. Rad.*, **12**, 650.
11. Falkenberg, G., Clauss, O., Swiderski, A. & Tschentscher, Th., 2001, *X-Ray Spectrom.*, **30**, 170.
12. Braun, S., Gawlitza, P., Menzel, M., Leson, A., Mertin, M. & Schäfers, F., 2007, *AIP Conference Proceedings*, **879**, 493.

Acknowledgements. The Synchrotron Light Research Institute's Graduate Scholarship under Contract No.GS-48-D05 and Graduate School, Department of Physics and Conference Grant for Ph.D. Student, Chulalongkorn University have supported this work.